Experimental and Monte Carlo determination of Gamma Spectrometry Efficiency

Pavel Dryak, Petr Kovář
Czech Metrology Institute
February 2009

Leading motive of our testing

The producer send the drawing after several requests, the drawing was for the type of the detector and it was clear that the parameters were nominal.

We asked for more precise information, we received this answer:

“I want to draw the attention of the customer to the fact that all information given about detector internal structure is strictly confidential.“

We do not believe the producer, we must verify his data and measure that data which the producer refuse to give us.

- The first model was based only on the CANBERRA information which we obtained from the drawing.

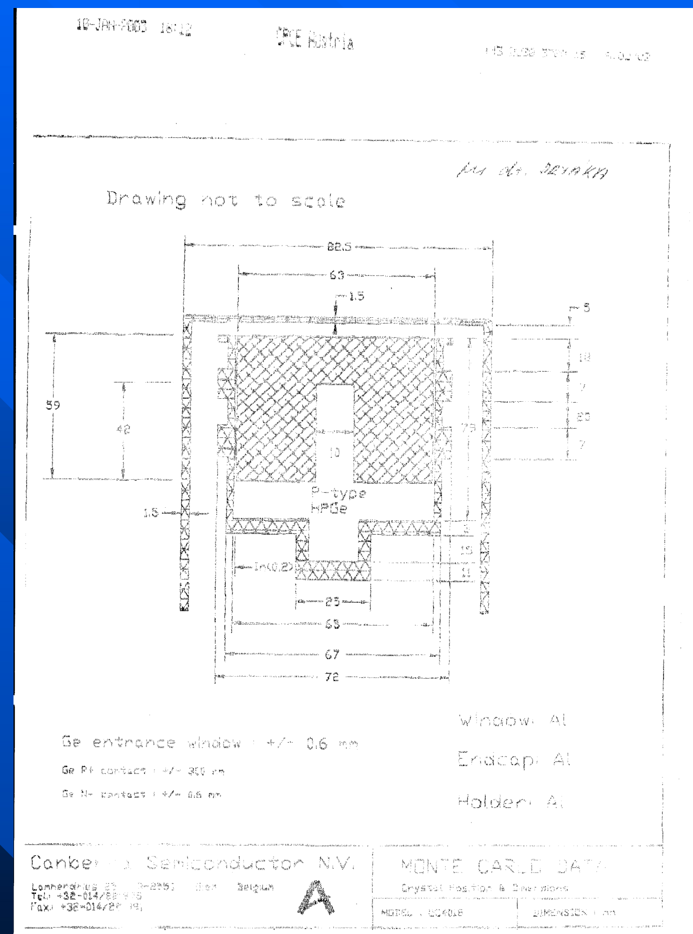

- Canberra refused any other information.

Resulting findings

- A precise model of HPGe detector type GC4018 (p type) was created for photon detection efficiency calculation using the MCNP 4A code.
- No experimental calibration point was used for determination of detector parameters.
- Radionuclide standards of CMI and PTB were used for model verification in the energy range 40 to 2615 keV for source-detector distance 24 cm. Deviations were very satisfactory.

What we did

The values of the parameters that describe the crystal and construction elements were verified or determined.

For the crystal diameter and thickness, the diameter and the radius of the inner hole, the distance between the crystal and the detector cap and the composition of the cap material the producer’s data were available.

The measured values agreed with the values if they were supplied by the producer.

- For the measurements of the properties of the internal detector structure the following methods were used:
  - Measurements of the density of germanium and aluminum on a detector crystal and on a piece of a cryostat belonging to an old detector,
  - Emission spectroscopy and X-ray fluorescence for measurements of the impurity concentrations in aluminum,
  - Radiography with X-rays and gamma rays from Ir-192, Cs-137 and Co-60 for measurements of the shape of the crystal, its position within the cap and the cryostat structure.
- The measurements of the dead layer thickness were made with collimated beams of gamma rays from Am-241.

Modeling steps

- The first version of model was based on the CANBERRA drawing. Calculated efficiencies (Co-60, Cs-137) were about 5% higher than experimental ones and efficiency for Am-241 was 4% lower.

- We improved step by step our knowledge of the detector parameters and we created better and better model.

- The important break-point-modeling after which was experiment and calculation closer were:
  - Identification of the size of the contact pin in the inner hole ;
  - Precise density of germanium and aluminum ;
  - Radius of the crystal edge ;
  - Precise shape of the crystal bottom ;
  - Increasing of MCNP-steps for the description of the motion of electron in germanium ;
  - Determination of the dead layer.

Identification of the size of the contact pin in the inner hole

- We used radiography pictures taken by Cs-137 and Co-60

- The measurement of any size contact pin whas done at the large screen.

  The Pt rod was used as a scale.

  The material of the pin is not important for the model, we estimated that it is brass.

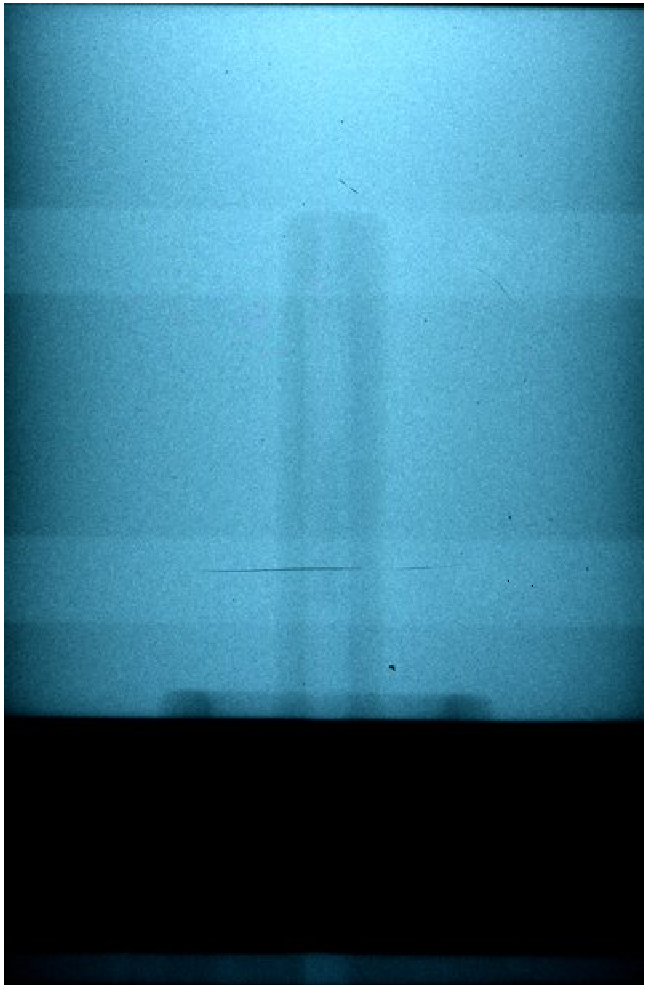

Precise density of Germanium

It was necessary to have a precise the density of Germanium

- The old Canberra Ge(Li) crystal was weighted in water. Now we know the density with very high precision : $\rho = 5.3255(5)$ g/ccm .
- Published values were 5.325 and 5.35.
- Calculated and experimental efficiencies became closer.

Precise density of Aluminum

- The Al density was tested by means of the old cryostat construction materials. The result was $\rho = 2.717\ (2)$ g/ccm.
- The Al purity was tested also on the old cryostat construction materials. Also a small piece of Al from our GC4018 cryostat was tested by the emission spectroscopy.

  We found 0.001% Cu, 0.1% Mg, 0.1% Si .
- The old construction materials were tested by RFT analysis.

  We found Cu from 0,005 to 0.01 %, Zn 0.002 to 0.005%.
- The impurities were neglected and we assumed Al to be highly pure with a density given by the one we measured.

Radius of the crystal edge

- We determined the radii from x-ray radiography pictures: upper edge 1.8 mm, lower edge 3mm.
- The measurement of any size was done at the large screen.
- The Pt rod was used as a scale.
- The uncertainty of any size was better then 2 %.
- Most of CANBERRA parameters were confirmed.

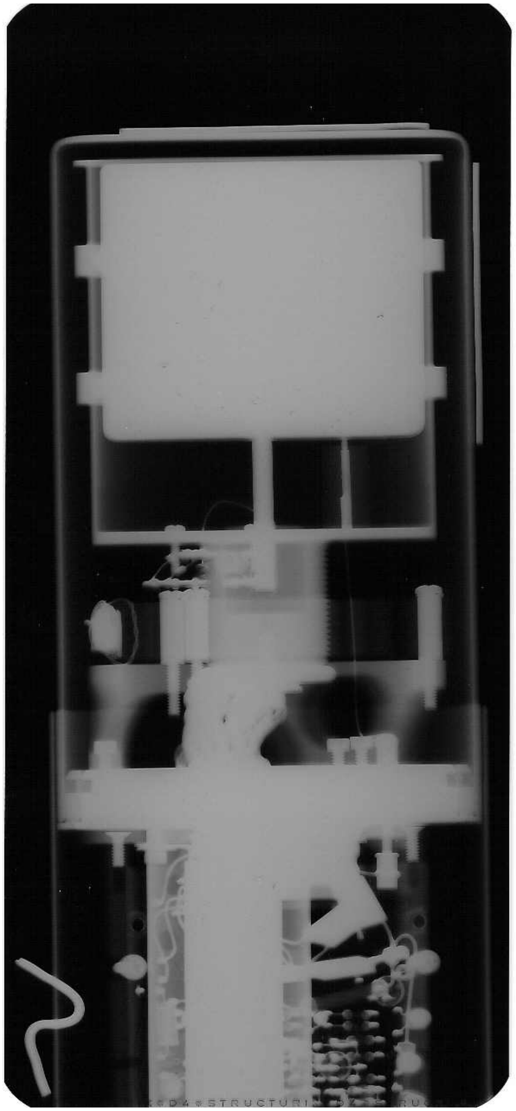

X-ray radiogram of the detector system

Precise shape of crystal bottom

- We discovered the complicated structure of the crystal bottom by radiography picture (see first picture).
- Again, the measurement of any size was done at the large screen. The Pt rod was used as a scale.

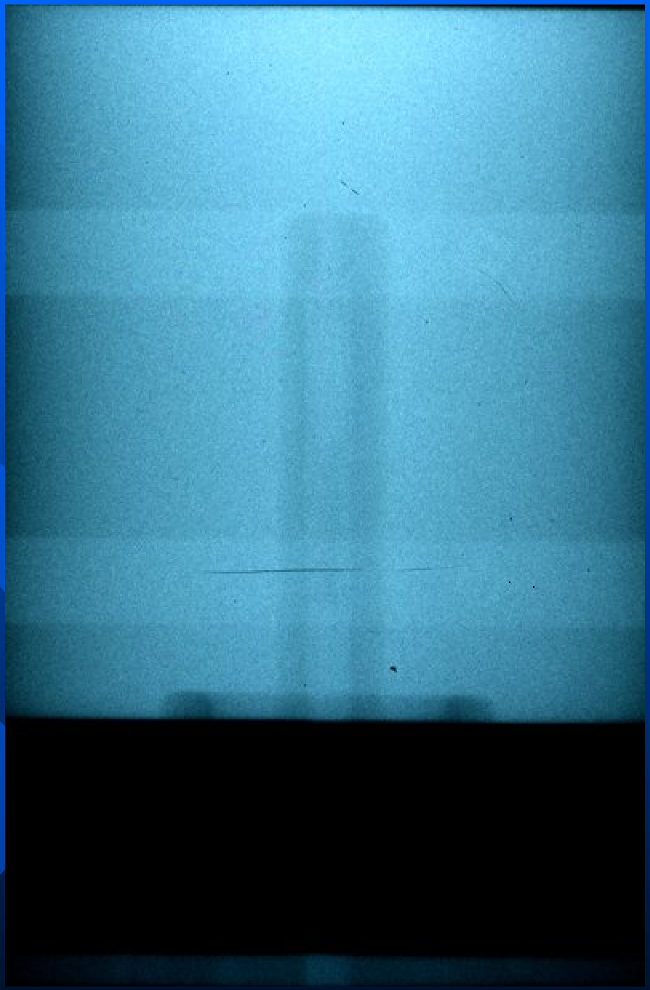

Increasing of steps for the description of the motion of electron in Ge

- The parameter "estep" in material cards was increased from 7 (by default) to 30 to achieve more realistic description of the electron motion through thin layers (mainly n+ contact in the hole):

```
c    x--- Material Cards ------------------------------------x
m1    32000 -1.0  estep=30            $ Germanium ro=5.3255
m2    13000 -1.0                      $ Aluminum  ro=2.717
```

- It seemed me that this modification decreased slightly the efficiency in the high energy region (in the good direction).

Determination of the dead layer thickness

- The thickness of the p+ contact: dead layer from the Canberra drawing is 0.6 mm.

- We made some experiments on the homogeneity of the dead layer over the top and side surfaces.

- We used a beam of 60 keV photons.

  The diameter of the beam was 1 mm.

- The collimator was moved along the top of the detector in two perpendicular directions with steps of 1 mm.

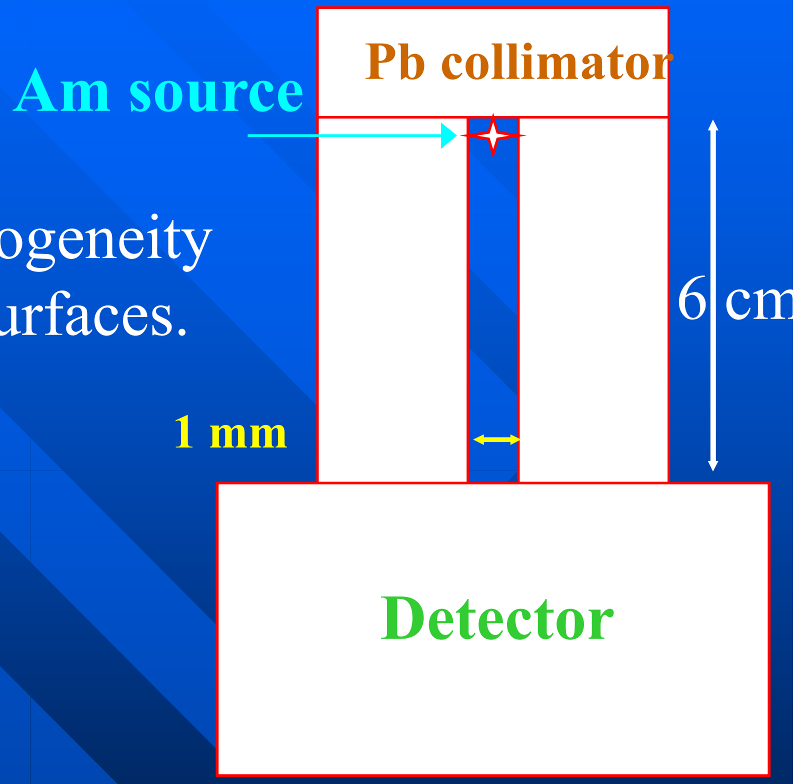

Horizontal profiles

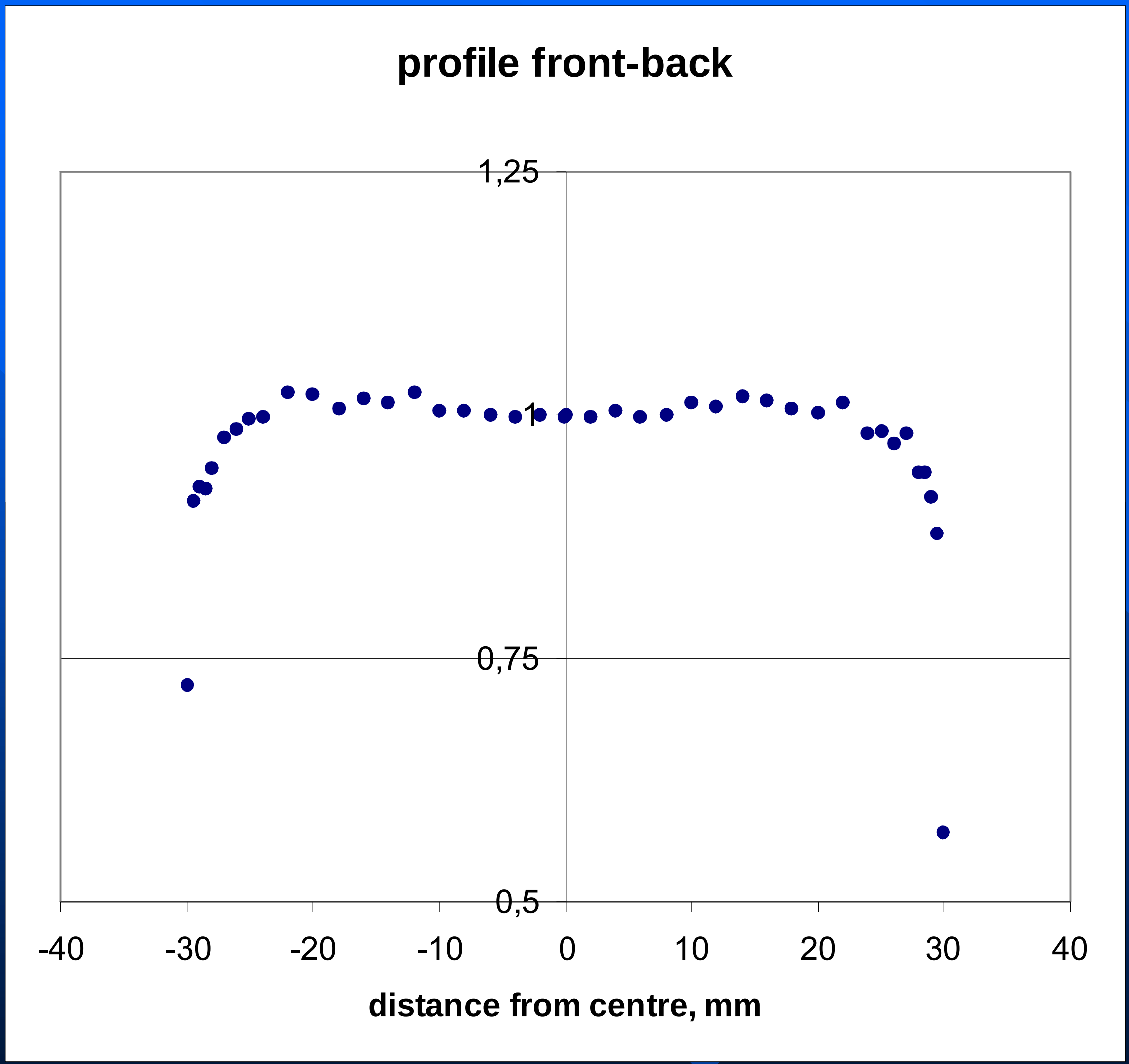

- The response is normalized to the center of the detector.

Horizontal profiles

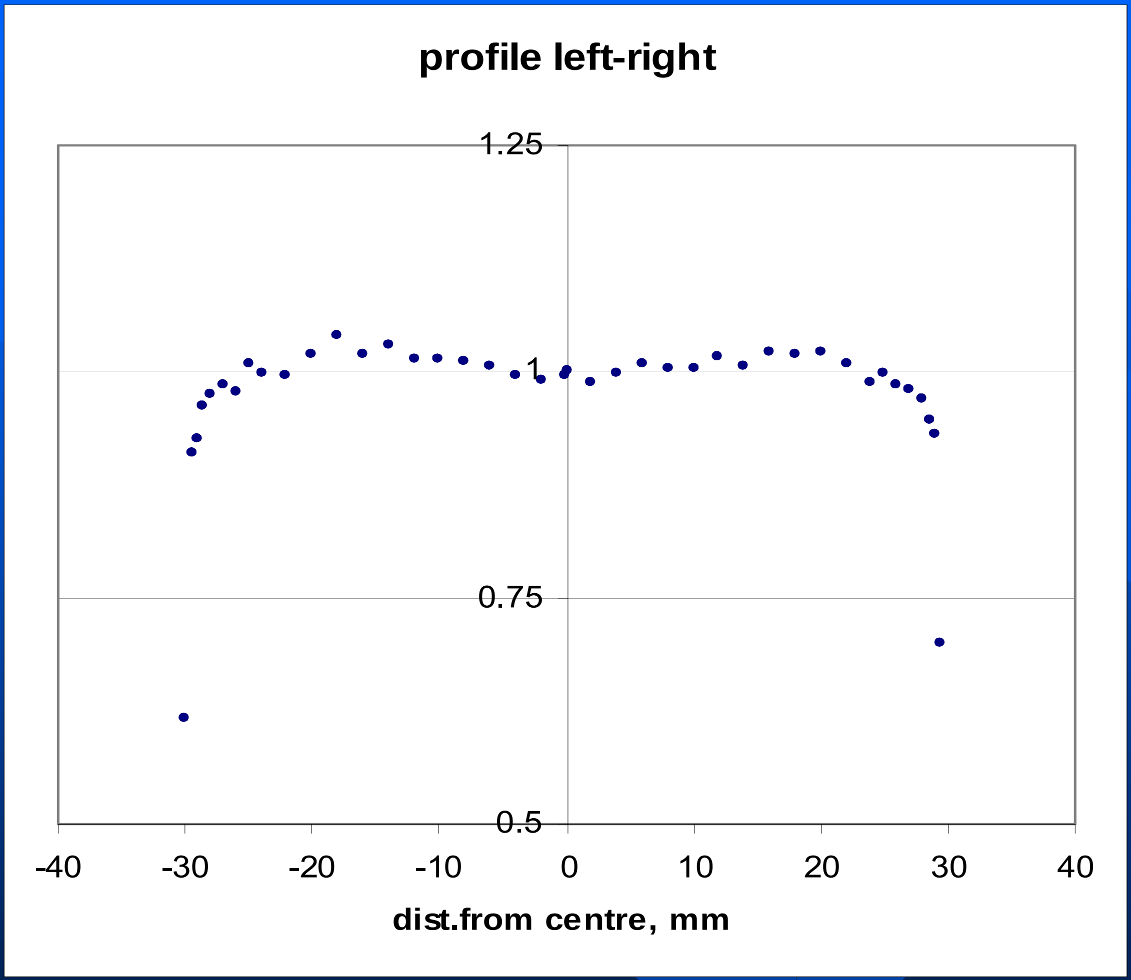

- It is evident from horizontal profiles that the dead layer in the central part of the top surface is thicker than in outer parts.

Vertical profiles

- The lower response at the top and bottom is due to rounding of the crystal, the lower response in places Al rings corresponds to the construction.

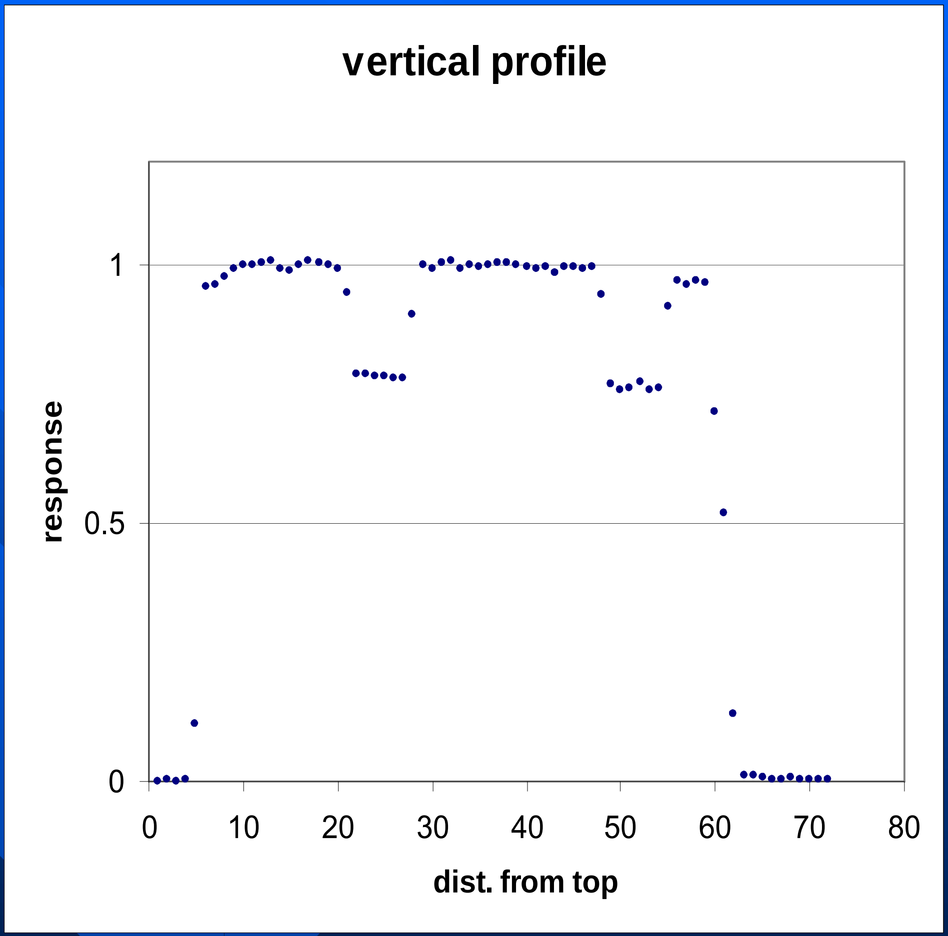

- The vertical profile indicates the homogeneity of the dead layer.

Determination of the dead layer thickness

- We also checked the response to 60 keV around periphery of detector (angle increment 30^{o}) in several distance from the top.
- This measurement indicated a homogeneous periphery but we discovered some absorbing material on one side, probably a grounded belt made from indium.
- A 100% to 51% degradation of the response to 60 keV was measured at this belt. The shielded area was determined to be 3x2.7=8.1 cm^2, (2.3% of the total area of the crystal surface).
- This additional absorption plays role in the marinelli geometry in the low energies region.
- The low segment of the belt was clearly seen under the crystal on some X-ray radiogram.
- The belt was included in the model.

Determination of the dead layer thickness

- The measurement of the dead layer thickness at the top surface was performed by two ways.

Method 1 :

- A hole with diameter 11.0(1) mm was in the Pb-shielding above central part of the crystal.
- It was possible to calculate the flux of 60 keV photons through the hole from Am-source with known activity in the distance about 50 cm.
- The dead layer in the center was estimated from the response to the known flux. The absorption in cryostat-material (2.1 mm Al) and air was included. The resulting dead layer was 0.540(10) mm.

Determination of the dead layer thickness

Method 2 :

- The measurements of the dead layer thickness was made with a collimated beam of gamma rays from Am-241.
- A beam with diameter 1 mm was directed to central point of the crystal top. The angles of the incidence were $0(1)^o$, $30^o(1)$, $60(1)^o$. The source and collimator distance from the central point was constant.
- The dead layer was estimated from the different peak areas corresponding to different angles. The absorption in cryostat-material (2.1 mm Al) was included.
- The result – 0.535(15) mm – was in an agreement with the value 0.540(10) mm for the central part of the detector.
- It would be possible to image the dead layer at the outer parts from the horizontal profiles. It should change in the limits 0.51 to 0.53 mm

Determination of the dead layer thickness

- Our first idea was that the model of the upper surface would consist of several quadratic surfaces (sphere + toroid + plane) corresponding to the experimental horizontal profile. Such model would lead to very thin layers.
- We were advised that MCNP does not work well with thin layers so we decided to suppose that the dead layer has constant thickness over top surface (and on the side surface too) of 0.5325(100) mm. This value is the numerical calculation result based on the profiles.
- All experiments were very interesting and the experiments concerning the dead layer were important to confirm our hypothesis that the dead layer is nearly homogeneous.

Parameters of model

- Final values of the detector system parameters :

Ge crystal parameters		
parameter	**value**	**method**
Ge density	(5.3255 ± 0.0005) g/cm^3	weighing in water
dead layer thickness	(0.5325 ± 0.0100) mm	gamma ray absorption
diameter	(62.5 ± 0.1) mm	X-ray radiography
length	(59.0 ± 0.1) mm	X-ray radiography
upper edge radius	(1.81 ± 0.02) mm	X-ray radiography
bottom edge radius	(3.91 ± 0.01) mm	X-ray radiography
bottom notch diameter	(27.43 ± 0.02) mm	Cs-137 radiography
bottom notch width	(5.14 ± 0.02) mm	Cs-137 radiography
bottom notch depth	(2.06 ± 0.02) mm	Cs-137 radiography

Parameters of model

inner hole parameters		
parameter	**value**	**method**
diameter	(10.0 ± 0.1) mm	Ir-192 radiography
depth	(42.0 ± 0.1) mm	Ir-192 radiography
contact pin diameter	(3.7 ± 0.1) mm	Ir-192 radiography
contact pin length	(7.0 ± 0.1) mm	Ir-192 radiography
P+ contact layer	300 nm	producer’s data

aluminum holder parameters		
parameter	**value**	**method**
Al density	(2.717 ± 0.001) g/cm^3	weighing in water
impurities	Mg (0.1 ± 0.05) % ; Sn (0.1 ± 0.05) % ; Cu ($\leq$ 0.01 %) Zn (< 0.005 %)	emission spectrometry X-ray fluorescence
entrance window	(0.6 ± 0.05) mm	X-ray radiography
diameter	(66.5 ± 0.1) mm	X-ray radiography
length	(82.0 ± 0.1) mm	X-ray radiography
thickness	(1.0 ± 0.1) mm	X-ray radiography
bottom thickness	(3.0 ± 0.1) mm	X-ray radiography
ring overlap	(2.5 ± 0.1) mm	X-ray radiography
bottom to crystal distance	(20.0 ± 0.1) mm	X-ray radiography
aluminum cryostat		
diameter	(82.5 ± 0.1) mm	X-ray radiography
thickness	(1.5 ± 0.1) mm	X-ray radiography
window to crystal distance	(5.0 ± 0.1) mm	X-ray radiography

Model of the detector

An axial cross-section through the detector model

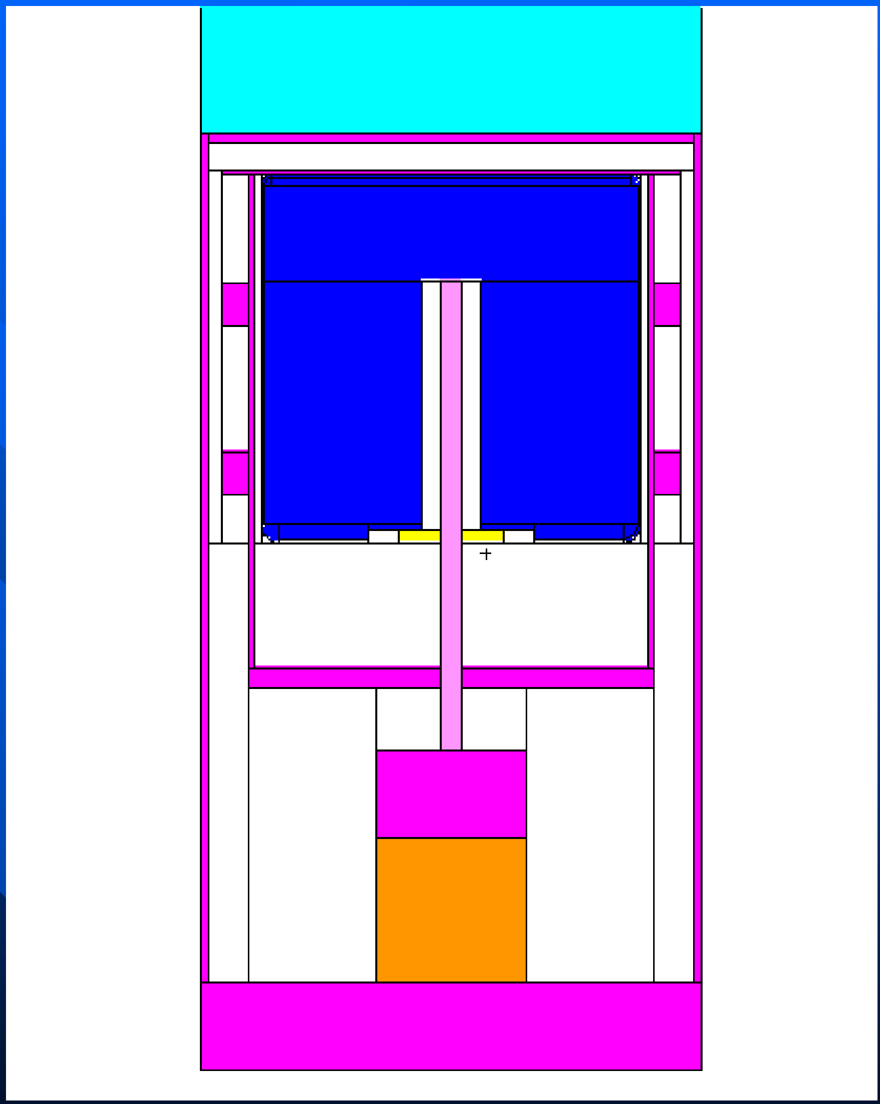

Ge - blue

air – light green

Al – violet

grass – light violet

teflon element – yellow

preamplifier - orange

Model of the detector

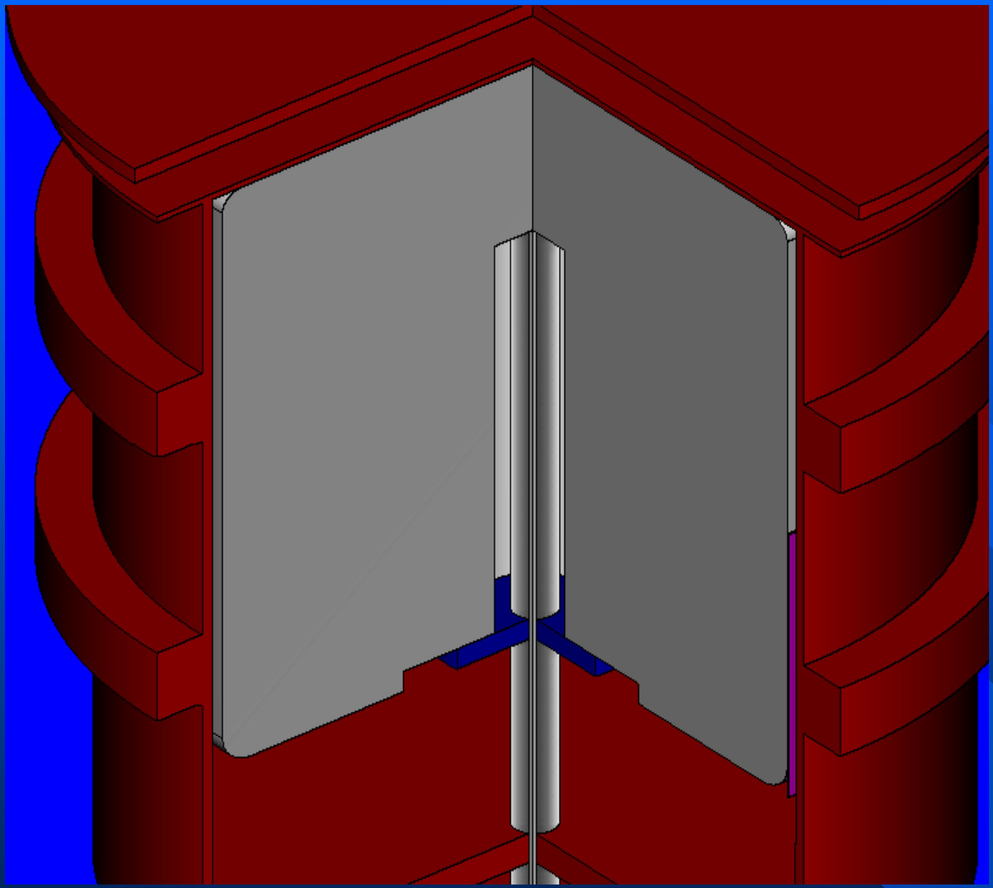

A view in the detector

Ge – grey

Al – red

teflon element – dark blue

grounded belt - violet

Comparison of calculated and experimental efficiencies for point sources at 25 cm

- Our model works well, see parameter $S = \varepsilon_{exp} / \varepsilon_{calc}$

Nuclide	E[keV]	ε_{calc}	U_c [%]	ε_{exp}	U_e [%]	S
Eu-152	39.91	4.6845E-04	0.12	4.6177E-04	0.77	0.9857
Am-241	59.54	1.7186E-03	0.07	1.7149E-03	0.58	0.9978
Am-241*	59.54	1.7185E-03	0.07	1.7138E-03	0.56	0.9973
Cd-109	88.04	2.4875E-03	0.08	2.4700E-03	0.55	0.9929
Eu-152	121.78	2.6294E-03	0.11	2.6087E-03	0.74	0.9921
Co-57	122.06	2.6308E-03	0.17	2.6157E-03	0.83	0.9943
Co-57*	122.06	2.6306E-03	0.17	2.6130E-03	0.54	0.9933
Ce-139	165.8	2.4603E-03	0.06	2.4470E-03	0.91	0.9945

Nuclide	E[keV]	ETAc	Uc [%]	ETAe	Ue [%]	S
Eu-152	244.7	1.9916E-03	0.07	1.9772E-03	0.75	0.9928
Eu-152	344.28	1.5390E-03	0.08	1.5353E-03	0.73	0.9976
Sr-85	514.00	1.1172E-03	0.08	1.1080E-03	0.81	0.9918
Cs-134	604.64	9.8467E-04	0.09	9.8320E-04	0.51	0.9985
Cs-137	661.65	9.1961E-04	0.1	9.0300E-04	0.84	0.9819
Cs-137*	661.66	9.1955E-04	0.1	9.1041E-04	0.52	0.9909
Eu-152	778.91	8.1319E-04	0.1	8.2026E-04	0.72	1.0087
Cs-134	795.84	8.0127E-04	0.11	8.0050E-04	0.59	0.9990
Mn-54	834.84	7.7272E-04	0.11	7.7250E-04	0.51	0.9997
Y-88	898.02	7.3185E-04	0.12	7.3758E-04	1.06	1.0078
Eu-152	964.01	6.9434E-04	0.11	6.9613E-04	0.72	1.0026

Nuclide	E[keV]	ETAc	Uc [%]	ETAe	Ue [%]	S
Co-60	1173.21	6.0036E-04	0.16	6.0220E-04	0.60	1.0031
Co-60	1332.47	5.4602E-04	0.16	5.4620E-04	0.60	1.0003
Co-60*	1173.21	6.0032E-04	0.16	5.9984E-04	0.45	0.9992
Co-60*	1332.47	5.4598E-04	0.16	5.4394E-04	0.45	0.9963
Eu-152	1408.04	5.2318E-04	0.14	5.2313E-04	0.76	0.9999
Y-88	1836.03	4.2197E-04	0.18	4.2100E-04	1.01	0.9977
Tl-208**	2614.53	3.0768E-04	0.21	3.0410E-04	1.01	0.9884
Na-24***	2754.03	2.9128E-04	0.19	2.9390E-04	1.00	1.0090

* PTB certified standards ; ** the source was 10g natural Th-232 ;
*** the source was not standardized by absolute method

Comparison of calculated and experimental efficiencies for marinelli geometry:

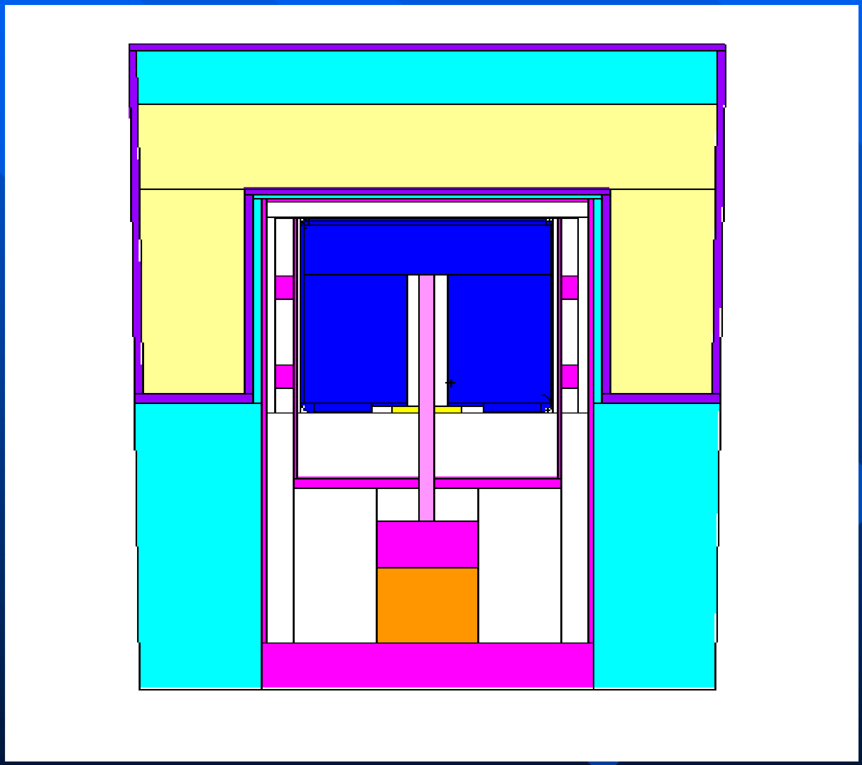

Calculated and experimental efficiency comparison for 1 liter Marinelli geometry

Energy, keV	ε calc x100	s calc %	ε exp x100	s exp %	calc/exp
59,54	2,0624	0,14	2,050	1	1,006
88,03	3,8280	0,06	3,746	2	1,022
122,06	4,4028	0,05	4,386	1	1,004
165,85	4,2527	0,05	4,167	2	1,021
279,19	3,1965	0,07	3,216	1	0,994
391,70	2,4931	0,08	2,529	2	0,986
514,00	2,0408	0,08	2,031	1	1,005
661,64	1,7023	0,08	1,694	1	1,005
898,04	1,3739	0,11	1,391	1,5	0,987
1173,23	1,1442	0,12	1,133	1,5	1,010
1332,50	1,0497	0,11	1,034	1,5	1,015
1836,03	0,8233	0,13	0,8199	1,5	1,004

Conclusion

- The exact description of the detector gives very good results of efficiencies.
- MCNP method can be used for the calibration of Ge detectors.